eNeuro

Research Article: New Research | Cognition and Behavior

Dorsal medial habenula regulation of mood-related behaviors and primary reinforcement by tachykinin-expressing habenula neurons

Dorsal medial habenula in mood regulation

Yun-Wei A. Hsu*, Glenn Morton*, Elizabeth G. Guy, Si D. Wang and Eric E. Turner

DOI: 10.1523/ENEURO.0109-16.2016

Received: 5 May 2016

Revised: 10 June 2016

Accepted: 22 June 2016

Published: 1 July 2016

Author Contributions: Y.-W.H., G.M., E.G.G., S.D.W., and E.E.T. designed research; Y.-W.H., G.M., E.G.G., and S.D.W. performed research; Y.-W.H., G.M., and E.E.T. analyzed data; E.E.T. wrote the paper.

Funding: NIH NIMH
R01MH093667

Funding: NIH NIDA
R01DA035838

Funding: NIH NIMH
F32MH098498

Funding: NIH NIDA
T32DA007278

Conflict of Interest: Authors report no conflict of interest.

This work was supported by National Institute Health Awards R01 MH093667 and R01 DA035838 to E.E.T. Y.-W.A.H. was supported by NIMH Training Award F32MH098498, and E.G.G. was supported by T32-DA007278.

*Y.-W.A.H. and G.M. contributed equally to this work.

Correspondence should be addressed to Eric E. Turner, Center for Integrative Brain Research, Seattle Children's Research Institute, 1900 Ninth Avenue, mail stop JMB-10, Seattle, WA 98101, USA, E-mail: eric.turner@seattlechildrens.org.

Cite as: eNeuro 2016; 10.1523/ENEURO.0109-16.2016

1 Manuscript Title (50 word maximum)

Dorsal medial habenula regulation of mood-related behaviors and primary reinforcement by tachykinin-expressing habenula neurons

2 Abbreviated Title (50 character maximum)

Dorsal medial habenula in mood regulation

3 List all Author Names and Affiliations in order as they would appear in the published article

Yun-Wei A. Hsu*, Glenn Morton*, Elizabeth G. Guy, Si D. Wang, and Eric E. Turner

*Equal contribution

4. Author Contributions: Each author must be identified with at least one of the following: Designed research, Performed research, Contributed unpublished reagents/ analytic tools, Analyzed data, Wrote the paper.

Y-W H Designed and Performed research and Analyzed data;

GM Designed and Performed Research and Analyzed data;

EGG Designed and Performed research;

SDW Designed and Performed research;

ET Designed research, Analyzed data, and Wrote the paper.

5. Correspondence should be addressed to (include email address)

Center for Integrative Brain Research
Seattle Children's Research Institute,
1900 Ninth Avenue, mail stop JMB-10,
Seattle, WA 98101
eric.turner@seattlechildrens.org

6. Number of Figures	8
7. Number of Tables	0
8. Number of Multimedia	0
9. Number of words for Abstract	239
10. Number of words for Significance Statement	119

11. Number of words for Introduction	500
12. Number of words for Discussion	1215

13. Acknowledgements

We thank Dr. Susan Ferguson for helpful comments on the experimental results and manuscript, Dr. Fritz Henn for helpful discussions, and Lely Quina for technical assistance. BAC transgenic mice were generated by the Gene Expression Nervous System Atlas (GENSAT) Project, NINDS Contracts N01NS02331 & HHSN271200723701C to The Rockefeller University (New York, NY). The content is solely the responsibility of the authors and does not necessarily represent the official views of the National Institutes of Health.

14. Conflict of Interest

'Authors report no conflict of interest'

15. Funding sources

This work was supported by National Institute Health Awards R01 MH093667 and R01 DA035838 to E.E.T. Y.-W.A.H. was supported by NIMH Training Award F32MH098498, and E.G.G. was supported by T32-DA007278.

Abstract

Animal models have been developed to investigate aspects of stress, anxiety and depression, but our understanding of the circuitry underlying these models remains incomplete. Prior studies of the habenula, a poorly understood nucleus in the dorsal diencephalon, suggest that projections to the medial habenula (MHb) regulate fear and anxiety responses, while the lateral habenula (LHb) is involved in the expression of learned helplessness, a model of depression. Tissue-specific deletion of the transcription factor Pou4f1 in the dorsal MHb (dMHb) results in a developmental lesion of this subnucleus. These dMHb-ablated mice show deficits in voluntary exercise, a possible correlate of depression. Here we explore the role of the dMHb in mood-related behaviors and intrinsic reinforcement. Lesions of the dMHb do not elicit changes in contextual conditioned fear. However, dMHb-lesioned mice exhibit shorter immobility time in the tail suspension test, another model of depression. dMHb-lesioned mice also display increased vulnerability to the induction of learned helplessness. However, this effect is not due specifically to the dMHb lesion, but appears to result from Pou4f1 haploinsufficiency elsewhere in the nervous system. Pou4f1 haploinsufficiency does not produce the other phenotypes associated with dMHb lesions. Using optogenetic intracranial self-stimulation, intrinsic reinforcement by the dMHb can be mapped to a specific population of neurokinin-expressing habenula neurons. Together, our data show the dMHb is involved in the regulation of multiple mood-related behaviors, but also support the idea that these behaviors do not reflect a single functional pathway.

Significance Statement

Our current understanding of neural circuits regulating mood states such as fear and depression is fragmentary. Recently, interest has grown in how the habenula, a poorly understood nucleus providing decending inputs to the tegmentum and raphe, may affect these behavioral states. We have employed mouse genetic models to study part of this system, the dorsal medial habenula (dMHb). Here we report that the dMHb is not, as previously proposed, required for normal acquisition of a conditioned fear response. Mice with genetic lesions of the dMHb show some profound effects in mood-related tests, but cannot be described strictly as “depressed” or “resilient”, suggesting

81 that at the circuit level, models of affective states are complex and do not report
82 identical phenomena.
83

Introduction

The habenula is a poorly understood brain nucleus lying dorsal to the thalamus. Recently, a series of studies has begun to explore the role of the habenula in behaviors related to mood regulation and stress. The habenula is divided into lateral (LHb) and medial (MHb) subnuclei, and the MHb can be further subdivided into a dorsal part (dMHb), containing excitatory neurons characterized by the expression of the tachykinin gene *Tac1*, encoding the neuropeptide substance P (SP), and a ventral part (vMHb), which contains glutamatergic neurons that also produce acetylcholine (Quina et al., 2009; Hsu et al., 2013). Anatomical studies have demonstrated that these subnuclei have distinct neural inputs and downstream targets in the brainstem. Past experiments have generally performed lesions of the entire habenula or its major output tract, the fasciculus retroflexus, and have assigned a wide variety of behavioral functions to the habenula (Lecourtier and Kelly, 2007), but this approach cannot resolve the specific functions of the habenula subnuclei.

Recent experiments targeting the specific input pathways from the septal nuclei to the vMHb and dMHb have implicated these circuits in the regulation of anxiety and fear responses, respectively (Yamaguchi et al., 2013). Nonetheless, it remains to be determined if the MHb subnuclei are directly involved in the expression of anxiety and fear responses. A pathway through the LHb has recently been shown to be involved in the expression of learned helplessness (Li et al., 2011; Li et al., 2013), a model of depression in which animals previously exposed to an inescapable aversive stimulus show diminished escape behavior when the stimulus is avoidable (Maier, 1984; Maier and Watkins, 2005; Duman, 2010). The LHb has well-established roles in reward and aversive functioning (Hikosaka, 2010; Proulx et al., 2014). The role of the LHb in mediating depression-like behaviors may thus be related to its roles in punishment (Matsumoto and Hikosaka, 2009), and aversion (Lammel et al., 2012; Stamatakis and Stuber, 2012). Although the MHb has distinct input and output circuitry from the LHb, recent evidence has shown that the MHb may also play a role in regulation of mood-related behaviors. Recently we have shown that mice with a developmental ablation of the dMHb, generated by targeted deletion of the transcription factor *Pou4f1* (dMHb^{CKO} mice), exhibit reduced voluntary wheel running activity (WRA), a possible correlate of

115 depression (Hsu et al., 2014). In addition, in contrast to the aversive effect of LHb
116 stimulation, the dMHb is intrinsically reinforcing in a self-stimulation paradigm (Hsu et al.,
117 2014), lending additional support for a role for the dMHb in the maintenance of hedonic
118 states.

119 In the present study we investigated whether neurons in the dMHb regulate
120 mood-related behaviors by testing $dMHb^{CKO}$ mice in models of fear (conditioned fear)
121 and depression (TST, learned helplessness). We found that mice with dMHb lesions do
122 not exhibit differences in contextual conditioned fear. The effects of dMHb ablation in
123 models of depression is significant, but cannot be interpreted simply as “depressed” or
124 “resilient”. Using a Cre-driver line that is specific for a tachykinin-expressing
125 subpopulation of dMHb neurons, we show that activation of these neurons is sufficient
126 to support self-stimulation reinforcement. Collectively, our data show that the dMHb is
127 involved in the regulation of multiple mood-related behaviors, but also suggest that
128 these behaviors are not mediated by a single neural pathway.
129

Materials and Methods

Transgenic mice used in the experiments. Mice with a tissue-specific null mutation of *Pou4f1* in the dMHb and control littermates used in this study were generated and genotyped as previously described (Hsu et al., 2014). The *Pou4f1* mutant mice used and their patterns of Pou4f1 transcription factor expression are listed in Figure 1A. Two strains of *Pou4f1* mutant mice were used: $Pou4f1^{tlacZ}$, a functionally null allele replacing the *Pou4f1* coding sequence with a β-galactosidase expression cassette (Quina et al., 2005, MGI:3512089), $Pou4f1^{flox}$, in which the principal coding exon of *Pou4f1* is flanked by loxP sequences (Hsu et al., 2014, MGI:5662420). The $Pou4f1^{flox}$ allele was excised using a Cre-recombinase expressing line, $Syt6^{Cre}$, (STOCK Tg(Syt6-Cre)KI148Gsat/Mmcd), a BAC transgenic generated by the GENSAT project (Gerfen et al., 2013, RRID:MMRRC_032012-UCD), and obtained as cryopreserved sperm from the Mutant Mouse Regional Resource Center of the University of California, Davis. Experimental mice with dMHb lesions and littermate controls were generated by crossing mice with the genotype $Pou4f1^{tlacZ/+}$, $Syt6^{Cre/Cre}$ with $Pou4f1^{flox/flox}$ mice to yield the genotypes $Pou4f1^{tlacZ/flox}$, $Syt6^{Cre/+}$ ($dMHb^{CKO}$) and $Pou4f1^{flox/+}$, $Syt6^{Cre/+}$ ($dMHb^{Ctrl}$) mice in equal ratios. The constitutive null $Pou4f1^{tlacZ}$ allele was used to generate $dMHb^{CKO}$ mice because the generation of animals with complete loss of Pou4f1 expression in the dMHb is more efficient if one allele is a constitutive null, and thus only one copy of the gene requires Cre-excision The presence of the *lacZ* gene product βGal also allows dMHb neurons to be identified by enzymatic staining or immunofluorescence in cells which no longer express Pou4f1 protein. The $dMHb^{CKO}$ mice show a profound loss of neurons in the dMHb due to postnatal cell death, while $dMHb^{Ctrl}$ mice do not show detectable loss of dMHb neurons (Figure 1B,C).

In order to isolate an effect of *Pou4f1* haploinsufficiency in the presence of an intact dMHb, mice that were homozygous or hemizygous for *Pou4f1* were generated by crossing male mice with the genotype $Pou4f1^{tlacZ/+}$, $Syt6^{Cre/Cre}$ with C57Bl/6 female mice to yield the genotypes $Pou4f1^{tlacZ/+}$, $Syt6^{Cre/+}$ ($Pou4f1^{+/-}$) and $Pou4f1^{+/+}$, $Syt6^{Cre/+}$ ($Pou4f1^{+/+}$) mice in equal ratios. In these genotypes the $Syt6^{Cre}$ allele has no effect because no floxed allele is present, but $Syt6^{Cre}$ was incorporated to maintain a consistent genetic background across all lines.

Mice for optogenetic studies of habenula function were generated by using the mouse line Ai32, which conditionally expresses the Channelrhodopsin-2 variant ChR2(H134R)-YFP from a modified floxed-stop Gt(Rosa)26Sor locus (Madisen et al., 2012, RRID:IMSR_JAX:024109). To generate mice expressing ChR2 in tachykinin-expressing neurons in the dMHb (dMHb^{ChR2} mice), Ai32 mice were interbred with mice bearing a Tac2^{IRESCre} allele, generated as a part of the Allen Institute Transgenic Characterization Project (Harris et al., 2014, RRID:IMSR_JAX:021878). Experimental mice from these crosses had the genotype Tac2^{IRESCre}/Ai32, and control mice bore the Ai32 allele, without Tac2^{IRESCre}. Mice expressing ChR2 in the vMHb (vMHb^{ChR2} mice) were generated by interbreeding Ai32 mice with mice bearing a Chat^{IRESCre} allele (Rossi et al., 2011, RRID:IMSR_JAX:006410) and have been previously described (Hsu et al., 2013). Tac2^{IRESCre} and Chat^{IRESCre} mice were obtained from Jackson Laboratories. Only male mice were used for the optogenetic experiments.

Analysis of gene expression. Immunofluorescence methods, including antibodies used to detect the *Pou4f1* protein Brn3a (RRID: AB_2314040), choline acetyltransferase (RRID: AB_2079751), substance P (RRID:AB_94639), and β-galactosidase (not in RRID), have been previously described (Hsu et al., 2014). Rabbit anti-mouse proNeurokininB was obtained from Novus Biologicals (RRID:AB_350516).

Contextual conditioned fear. Fear conditioning was performed in a 13cm by 17cm compartment (one compartment of ENV-3013, Med Associates, equipped with grid floor ENV-3013BR). The grid floor was connected to a shock scrambler (ENV-414S, Med Associates) set to 0.40mA. The Activity Tracking function of Noldus Ethovision XT 10 was used to analyze freezing behavior, which is defined by the absence of observable movement, except for respiration. On day 1, mice were allowed to acclimate to the chamber for 3 minutes, followed by the delivery of a 1s shock every minute for 6 minutes. To the extent possible, this training procedure was designed to reproduce the methods used in a prior study (Masugi et al., 1999; Yamaguchi et al., 2013). On the second day of the procedure animals were returned to the same compartment for 6 minutes in the absence of shocks in order to assess the contextual conditioned fear response.

We implemented automated scoring of freezing behavior based on a published method using an earlier version of Noldus Ethovision (Pham et al., 2009). Automated analysis of the video derived the image of the subject in each video frame (frame rate 30 s^{-1}, duration 33.33ms). A moving average of the subject image in the previous three video frames was then compared to the current frame, and the subject was determined to be immobile if the image area occupied by the subject in the current frame was changed (displaced, or altered in size or shape) from the moving average by less than 0.02%. The activity was scored as freezing if immobility lasted longer than 0.5s, corresponding to 15 consecutive samples of immobility at the video frame rate of 30 s^{-1}. Reliability of the automated video analysis of freezing behavior was confirmed by manual scoring of test videos of control mice by two human raters blind to the automated scoring results.

Tail Suspension Test. The test was performed using inverted U-shaped acrylic stand (18" x 18", with a 4" wide horizontal arm), placed in an isolation chamber with a video camera positioned to include 1.5 inches of the horizontal arm and the entire length of the subject within the field of view. At the start of the trial, subjects were suspended from the crossbar using tape placed one inch from the tip of the tail. Although C57BL/6 mice have been observed to climb their tails when performing this test, this behavior was not observed using this apparatus. A 6-minute video was recorded and analyzed in Noldus Ethovision XT 10.0 using Activity Tracking. Each recorded video frame was compared to the previous frame (frame rate 30 s^{-1}, duration 33.33ms) and the mouse was determined to be immobile for that period if less than 5% change was observed from one frame to the next.

Learned helplessness and active avoidance. The learned helplessness protocol consisted of a training session or sessions in which mice were exposed to inescapable shock stimuli, followed by analysis of the learned helplessness response using active avoidance in a two-way shuttle box. Training consisted of 360 shocks of random duration between 1-3s and random inter-stimulus interval of 1-15s, delivered over approximately one hour, using Noldus Ethovision XT 10.0. Active avoidance was assessed using 60 escape trials on the following day, or after three weeks to assess the persistence of the learned helplessness response.

Learned helplessness training was performed in a 13cm by 17cm chamber (either of the main compartments of ENV-3013, Med Associates). Chambers were equipped with conductive grid and rod floors connected to a shock scrambler (ENV-414S, Med Associates) set to 0.40mA. The active avoidance test was performed in a 42cm x 16.5cm center channel modular shuttle box chamber (ENV-010MC, Med Associates) equipped with a video monitoring and analysis system (Noldus Ethovision XT 10.0). The grid floor was connected to the same scrambler used for training and set to 0.40mA. Sixty escape trials were performed, each consisting of a 4.5 kHz tone followed by a shock. The tone preceded the onset of the shock by 2s and continued until the shock event stopped. The maximum duration of each shock was 4s, and the shock could be avoided by crossing to the opposite side of the compartment during the tone, or stopped by crossing during the shock. A random intertrial interval of 19-29s was used between trials. Latency to escape was scored as 0 if the animal successfully escaped during the tone before onset of the shock. Otherwise, latency time was calculated from shock onset to the time of escape. A maximum score of 4 was given if the animal failed to escape the shock. The mean latency to escape was calculated over the sixty trials for each mouse.

Over the course of the experiments we observed that a small number of mice adopted an unintended strategy for shock avoidance in which they straddled the midline of the shuttle box. This behavior caused the video analysis to dither and falsely report a very high frequency of midline crossings, which was easily identified on analysis of the data. The shuttle box arenas defined in the video analysis software were modified in later experiments such that the mouse was required to travel at least 4cm beyond the midline in order to avoid or terminate the shock. This modification somewhat increased escape latency because of the increased distance traveled. Cohorts of 10 C56Bl/6 male mice were used to assess the effect of this change in the arena boundaries on the measurement of the learned helplessness response. Significant differences were observed between trained and naïve animals using both arena structures.

Accelerating rotarod. A specialized apparatus (Rotamex-5, Columbus Instruments) was used to test rotarod performance as previously described (Hsu et al., 2014). Briefly, before testing all mice were trained on a fixed-speed protocol at 4 rpm

until they could stay on the rod for 30 seconds. On the same day as the training sessions, mice underwent four 5-minute accelerating rotarod trials. In each trial, the rotarod accelerated from 4 rpm to 40 rpm at the rate of 1 rpm every 8 seconds, then remained at 40 rpm until the end of the trial. The principal outcome was the time (latency) until the mouse fell from the rod. Mice were given at least 15 minutes of rest in between each trial. To calculate the average latency to fall for each mouse, the lowest of four values was discarded.

Optogenetic intracranial self-stimulation (ICSS). ICSS reinforcement by the dMHb was tested in an operant chamber (ENV-307W, Med Associates) equipped with two nosepoke receptacles (ENV-313W, Med Associates). Responses were recorded through four training and four reversal sessions. *Training sessions.* Mice underwent four 45 min ICSS sessions in which a randomly assigned active nosepoke receptacle was associated with the delivery of laser stimulation to the dMHb via an implanted fiber optic cannula (above), and the inactive receptacle did not deliver a stimulus. A 1:1 fixed response: reward ratio was used. The reward consisted of a two-second train of 25ms light pulses, delivered at 20 Hz and 8mW with a 473 nm laser, followed by a two second time-out period. Nosepokes during the period of laser stimulation and time-out were recorded but did not trigger a reward. Nosepokes on the inactive receptacle were also recorded. *Reversal sessions.* The reinforcing effect of ICSS was confirmed in four reversal sessions during which the active receptacle was switched to the opposite side, using the same session structure.

Real-time place preference. RTPP studies were conducted in a two-chamber place-preference box (ENV-010MC, Med Associates) in which mice received light stimulation in one side, and could move freely between compartments. Recording and laser stimulation were controlled with EthoVision XT using center point tracking. Sessions were initiated by placing the mouse in the center of the apparatus. The mice were then given free access to both chambers for 15 minutes. When the mouse entered the active chamber, the 473 nm laser was activated, delivering 25ms light pulses at a 20Hz and 8 mW of total power continuously until the mouse crossed over to the inactive chamber. Conversely, upon entering the inactive chamber, the laser remained off until the mouse entered the active chamber. Active and inactive chamber occupancy

and total distance traveled were then calculated for each 5 minute interval of the 15 minute session.

General statistical methods. Statistical analyses were conducted using unpaired two-tailed t-tests, two-way ANOVA or two-way repeated measures ANOVA with Tukey's or Bonferroni's post-hoc analyses in GraphPad Prism 6 (GraphPad Software). Results are presented as means ± SEM. We also considered that in this paper and in a prior paper (Hsu et al., 2014), we compared dMHb CKO mice and controls in multiple behavioral models that use a motor output measure as a model of depression/behavioral despair.. These tests include learned helplessness, the persistence of learned helplessness, and the tail suspension test in the present study, and the forced swim test in the prior study. In the prior study we also interpreted a deficit in rotarod function as possibly related to behavioral despair. Given that five independent tests were applied, Bonferroni correction for the number of tests suggests that a threshold significance value of $p< 0.01$ rather than $p<0.05$ should be used. Using this more stringent standard, the effect of genotype is still significant for learned helplessness, persistence of learned helplessness, tail suspension, and rotarod tests. The effect in the forced swim test was not significant at $p<0.05$.

Results

The conditioned fear response is not affected by developmental loss of dMHb neurons. Recently, lesion studies of the specific septal inputs to the dorsal and ventral MHb have shown that the septohabenular pathway is involved in the regulation of anxiety and fear (Yamaguchi et al., 2013). Specifically, lesions of septal inputs to the dMHb increased freezing behavior in the training phase of a conditioned fear paradigm. (Contextual conditioned fear *per se* was not tested). To test for direct involvement of the dMHb in fear conditioning we assessed fear acquisition and the contextual fear response using $dMHb^{CKO}$ mice and controls. The $dMHb^{CKO}$ mouse bears a dMHb-specific deletion of the *Pou4f1* coding sequence, and shows a nearly complete developmental loss of dMHb neurons (Figure 1). Both the $dMHb^{Ctrl}$ and $dMHb^{CKO}$ mice exhibited the same amount of freezing on the training day (day1) during shock administration (2-way ANOVA, genotype x trial, effect of genotype, $F_{(1,20)} = 0.11$, $P = 0.74$; Figure 2A, time 4 to 9 min), and time spent in freezing increased with each subsequent shock administration (effect of trial, $F_{(5,100)} = 18.48$, $P < 0.0001$). Contextual fear response was tested on day 2 by placing the mice in the same environment without shock administration (Figure 2B). Both genotypes exhibited the same amount of freezing (2-way ANOVA: effect of genotype, $F_{(1,20)} = 0.15$, $P = 0.70$), with increasing freezing behavior as the test progressed (effect of trial, $F_{(5,100)} = 8.45$, $P < 0.0001$). Finally, we examined the time course for the extinction of conditioned fear response. Fear extinction was tested over three subsequent days of exposure to the environment without shock stimuli (Figure 2C). The freezing response gradually diminished in a similar manner for both genotypes (2-way ANOVA: effect of genotype, $F_{(1,20)} = 0.20$, $P = 0.66$; effect of day: $F_{(2,40)} = 21.91$, $P < 0.0001$). Post-hoc analyses revealed that both the $dMHb^{Ctrl}$ and $dMHb^{CKO}$ mice spent significantly less time freezing starting at two days post-training. Thus we conclude that dMHb ablation has no significant effect on acquisition of the fear response, and no effect on contextual conditioned fear or its extinction.

***Pou4f1* gene dosage affects learned helplessness in an active avoidance model.** Another model for assessing depression-like behavioral changes in rodents is learned helplessness. In this paradigm, animals are exposed to stress in the form of

inescapable shocks, and the uncontrollability of the stressful stimulus is thought to generate a learned helplessness behavior in which animals subsequently fail to escape an aversive stimulus in a different environment (Maier, 1984). Like the FST and TST, learned helplessness has been used to predict antidepressant response (Duman, 2010). In the implementation of learned helplessness used here, mice were administered inescapable shocks during one training session in an apparatus used exclusively for the training. Mice were then tested 24hr later for active avoidance in a separate two-way shuttle box to assess the learned helplessness response (Chourbaji et al., 2005). The mice were also tested three weeks later to determine the persistence of learned helplessness.

Both dMHb^{CKO} and dMHb^{Ctrl} mice that received inescapable shocks during training took longer to escape the shocked compartment on the testing day compared to unshocked mice (two-way ANOVA: genotype x treatment, effect of treatment, $F_{(1,47)}$ = 49.50, $P < 0.0001$; Figure 3A), and mice also showed a significant difference in escape latency between genotypes (effect of genotype, $F_{(1,47)} = 11.39$, $P = 0.0015$). Post-hoc analyses indicate that while no difference was observed between the dMHb^{CKO} and dMHb^{Ctrl} mice that did not receive inescapable shock training ($P = 0.70$), dMHb^{CKO} mice that received inescapable shocks had longer escape latency compared to shocked dMHb^{Ctrl} mice ($P = 0.0029$). Thus the genetic lesion in dMHb^{CKO} mice rendered them more vulnerable to the development of learned helplessness behavior. The learned helplessness phenotype persisted three weeks after shock training (Figure 3B), and there was a significant difference attributable to shock administration ($F_{(1,47)} = 15.38$, $P = 0.0003$) and genotype ($F_{(1,47)} = 16.99$, $P = 0.0002$). Post-hoc analyses suggest that this is due to the persistence of learned helplessness response retained by the learned helplessness dMHb^{CKO} mice. We also examined the effect of extended training and determined that learned helplessness response of the dMHb^{CKO} and dMHb^{Ctrl} mice converged after three days of inescapable shock administration ($t_{(18)} = 1.20$, $P = 0.24$; Figure 3C).

Although the most obvious explanation for the sensitization to learned helplessness in dMHb^{CKO} mice is the nearly complete loss of dMHb neurons in these animals, these mice possess one conditional *Pou4f1* allele (*Pou4f1*^{flox}) and one *Pou4f1*

null allele (*Pou4f1*^{tlacZ}, Methods), and are thus globally hemizygous for *Pou4f1*. In order to determine whether the observed learned helplessness phenotype resulted from the developmental loss of dMHb neurons, or could be a general effect of *Pou4f1* haploinsufficiency, we also examined learned helplessness in Pour41$^{+/-}$ mice and Pou4f1$^{+/+}$ controls. After one day of inescapable shock administration, Pou4f1$^{+/-}$ mice took longer to escape the shocked compartment during the active avoidance test compared to Pou4f1$^{+/+}$ mice ($t_{(30)} = 2.97$, P = 0.0059; Figure 3D). As observed in the dMHb^{CKO} mice, the learned helplessness response persisted in the Pou4f1$^{+/-}$ mice three weeks after the initial shock administration ($t_{(30)} = 3.78$, P = 0.0007; Figure 3E). We conclude that the increased susceptibility to induction of learned helplessness behavior in Pou4f1-deficient mice is not exclusively dependent on the ablation of dMHb neurons.

dMHb^{-}lesioned mice exhibit prolonged escape behavior in the tail suspension test. Previously reported experiments have shown that developmental loss of the dMHb does not increase immobility time during the forced swim test, a model of stress response and depression (Duman, 2010; Hsu et al., 2014). Here, we assessed the behavior of dMHb^{CKO} mice using another model of depression, the tail suspension test (TST, Steru et al., 1985; Cryan et al., 2005). Rodents suspended by their tails will initially struggle to escape, but eventually stop and become immobile. The time that the mice spend immobile in a trial of fixed duration is recorded as the principal outcome of the test. dMHb^{CKO} mice showed lower immobility time compared to dMHb^{Ctrl} mice during the six-minute test ($t_{(18)} = 3.47$, P = 0.0027; Figure 4A).

In order to test whether the TST phenotype could be due to haploinsufficiency of *Pou4f1*, rather than the dMHb lesion observed in dMHb^{CKO} mice, we also performed the TST on cohorts of matched Pou4f1$^{+/-}$ and Pou4f1$^{+/+}$ mice (Figure 4B). No difference in TST immobility time was observed between Pou4f1$^{+/-}$ and Pou4f1$^{+/+}$ mice ($t_{(30)} = 0.84$, P = 0.41). Thus we conclude that the developmental loss of the dMHb mediates the reduced TST immobility observed in dMHb^{CKO} mice.

Pou4f1 haploinsufficiency does not affect rotarod and voluntary wheel running performance. A prior study has shown that dMHb^{CKO} mice have a deficit in the accelerating rotarod test, with a markedly shortened latency to fall from the device, and a reduction in voluntary wheel running activity (WRA, Hsu et al., 2014). Although

the rotarod is usually used to assess motor deficits, other tests of motor function in these mice, including open field locomotion, gait, and balance beam performance, were largely normal (Hsu et al., 2014). For this reason it was concluded that the deficits in rotarod and WRA in dMHb^{CKO} mice likely resulted from a loss of motivation or reinforcement, rather than a deficit in motor function *per se*. Here, however, we have shown that *Pou4f1* haploinsufficiency can contribute to a mood-related phenotype, learned helplessness. Thus, to determine if *Pou4f1* haploinsufficiency affects rotarod performance, we repeated this test in Pou4f1$^{+/-}$ and Pou4f1$^{+/+}$ mice. Both genotypes have similar fall latency in the rotarod test (t-test, $t_{(30)} = 1.42$, $P = 0.17$; Figure 4C), confirming that the reported deficit in rotarod performance in dMHb^{CKO} mice results from the developmental loss of dMHb neurons, not from *Pou4f1* haploinsufficiency.

Experiments to be published elsewhere demonstrate that WRA does not differ significantly between Pou4f1$^{+/-}$ and Pou4f1$^{+/+}$ mice (Y.-W. Hsu, in preparation), and thus that the WRA deficit in dMHb^{CKO} mice is also specifically related to dMHb ablation.

Tachykinin-expressing dMHb neurons mediate ICSS reinforcement. The dMHb is characterized by the expression of the tachykinin genes Tac1 (encoding SP), expressed exclusively in this subnucleus (Figure 5A, Quina et al., 2009), and Tac2 (encoding NKB), which is expressed in the dMHb and vMHb (Figure 5B). Here we wished to test whether these tachykinin-expressing dMHb neurons are sufficient to mediate ICSS reinforcement, potentially linking the MHb to the behavioral effects ascribed to tachykinins and their receptors.

In search of an optogenetic ICSS model, we examined reporter expression driven by a Tac2^{IRESCre} transgenic line generated as part of the Allen Institute Transgenic Characterization Project (Harris et al., 2014). These mice were crossed with a Cre-dependent reporter line, *Ai32*, that conditionally expresses a ChR2-eYFP fusion protein (Madisen et al., 2012). Surprisingly, reporter expression more strongly resembled that of Tac1 mRNA than Tac2 mRNA, in that it was largely restricted to a subset of neurons in the dMHb (Figure 5C). Expression of eYFP was rarely observed in the vMHb, as defined by the expression of the cholinergic marker choline acetyltransferase (ChAT, Figure 5D). PCR with allele-specific oligos confirmed the correct insertion of the targeted transgene at the *Tac2* locus. We note that Allen

Institute database *in situ* hybridization data for Tac2^{IRESCre} crossed with another reporter line, Ai14, shows the same pattern of reporter expression, restricted to the dMHb (Figure 5E). Finally, we note that an independently generated Tac2^{Cre} driver line, generated by replacement of the Tac2 gene rather than targeting of an IRES-Cre to the 3'-untranslated region of the transcript, shows a similar pattern of expression, primarily in the dMHb (Mar et al., 2012). Consistent with the pattern of marker expression driven by Tac2^{IRESCre} in the dMHb, selective innervation by labeled fibers is found in the lateral nucleus of the IP (IPL, Figure 5F-H), in which pre-synaptic dMHb fibers are marked by the expression of the Tac1 gene product SP (Figure 5I,J) and the Tac2 gene product NKB (Figure 5K). Tac2^{IRESCre} labeled fibers are relatively sparse in the IPR/IPC, where Chat-immunoreactive fibers originating in the vMHb are located. It is not known why Tac2^{IRESCre} shows a strong preference for the dMHb and its efferent target the IPL, but we conclude that Tac2^{IRESCre} is a suitable model system for selective manipulation of tachykinin (Tac1/Tac2) expressing neurons in the dMHb.

In order to test ChR2 function in Tac2^{IRESCre}, Ai32 (dMHb^{ChR2}) mice, we first evaluated light-evoked neural activity in the dMHb using cell-attached recording in acute brain slices (Figure 6A,B). Of the six light-responsive dMHb neurons sampled, one was spontaneously active at ~4Hz, one was spontaneously active at <1Hz, and four were silent until exposed to light pulses. All six recorded neurons could be entrained with complete fidelity to a train of pulses delivered at 10Hz; in some neurons entrainment with a 20Hz pulse train resulted in omission of some spikes (Figure 6B). The waveforms of spontaneous and evoked spikes were very similar (Figure 6A, expanded view).

To test whether dMHb neurokinin-expressing neurons mediate intrinsic reinforcement, we employed an optogenetic ICSS protocol. dMHb^{ChR2} mice were implanted with a bilateral optical fiber cannula positioned just dorsal to the dMHb (Figure 7). To determine if vMHb neurons, identified by the expression of acetylcholine as a co-transmitter, might mediate ICSS reinforcement, we also implanted Chat^{Cre}, Ai32 (vMHb^{ChR2}) mice. The neurons of vMHb^{ChR2} mice have been previously shown to have light responses similar to those shown here for dMHb^{ChR2} neurons in acute brain slices

(Hsu et al., 2013). Littermate mice lacking a Cre driver were implanted with optical fibers and used as controls for both optogenetic genotypes.

ICSS was evaluated in four training sessions in which mice were presented with a two nosepoke receptacles, one of which delivered a two-second train of light pulses upon entry, and one of which was inactive. dMHb^{ChR2} mice developed a preference for the active receptacle on the first training day, which persisted through four days of training (Figure 6C,F). The cohort of dMHb^{ChR2} mice then underwent four sessions in which the active receptacle was reversed. One day (day 5) was required for extinction of the response to the previously active receptacle, and by day 6 of training, a preference for the newly active receptacle was established. In contrast, vMHb^{ChR2} mice (Figure 6D,F) and control mice (Figure 6E,F) did not establish a significant preference over four days of training. ICSS using a nosepoke response is not an effective measure of aversion, since both a neutral stimulus and an aversive one may elicit no response. For this reason we tested possible aversion to light stimulation in dMHb^{ChR2} mice in a real-time place preference paradigm (Hsu et al., 2014). No aversive or reinforcing response to dMHb stimulation was detected in this paradigm (Figure 8). We conclude that the reinforcing effect of MHb stimulation is specifically conferred by activation of neurokinin-expressing dMHb neurons, and that ICSS is more effective at detecting this effect than place preference.

Discussion

Fear conditioning, the induction and learning of threat responses in rodents, is a widely used model of human stress-related disorders. Studies of the neural pathways underlying contextual and cued (Pavlovian) fear conditioning have focused on core circuitry involving the amygdala (Dejean et al., 2015; Keifer et al., 2015), with the integration of hippocampal and frontal circuits in contextual conditioning (Maren et al., 2013; Rozeske et al., 2015), and the periaqueductal gray in mediating the freezing response. Although the dMHb is not part of this amygdala-centered circuitry known to be involved in conditioned fear, a recent report suggests involvement of the septohabenular pathway in fear behavior (Yamaguchi et al., 2013). In this study, immunotoxin-mediated cell targeting was used to ablate neurons in the bed nucleus of the anterior commissure (BAC), part of the septal complex, that project specifically to the dMHb. BAC-ablated mice showed increased freezing response during fear training, but the effect on conditioned fear was not reported. Here we have used a contextual conditioning protocol, without a specific cue, to reproduce the original study to the extent possible. Our results demonstrate that the dMHb is not essential for the acquisition of acute fear or for the contextual conditioned fear response. Further understanding of the septohabenular circuitry may shed light on why the fear response was not affected in our study. It is possible that ablation of the BAC may have effects on fear behavior that are not mediated by the dMHb.

Consistent with our results, lesions of the entire habenula (MHb + LHb) in mice show no net effect on conditioned fear (Heldt and Ressler, 2006). However, a recent study has shown that cue conditioned fear is modulated by cannabinoid receptors in the MHb (Soria-Gomez et al., 2015). This effect is attributed to vMHb neurons that use acetylcholine as a co-transmitter, which are intact in the mice used in the present study (Figure 1) rather than the dMHb. Thus to date there is no evidence for a direct role for the dMHb in fear conditioning.

Here and in a prior study (Hsu et al., 2014) we have examined the effect of dMHb ablation in several widely-used models of depression, including the Porsolt forced swim test (FST), the TST, the sucrose preference test, and learned helplessness. Ablation of the dMHb had no discernable effect on the FST (Hsu et al., 2014), yet in the present

study, dMHb^{CKO} mice show reduced immobility in the conceptually-related TST, a result that could be interpreted as an antidepressant response. These tests are conceptually associated based on the common concept of "behavioral despair", originally applied to the FST, in which rodents initially attempt to escape an adverse situation, then become passive and relatively immobile. The widely used animal models of depression have been linked to mood states by their face validity and their value in predicting antidepressant responses (Cryan and Mombereau, 2004; Duman, 2010). However, antidepressants work on neurotransmitter systems with broad CNS effects. Because the FST and TST involve different stimuli and different locomotor responses, there is no reason to assume that these tests will always have concordant results in transgenic models that affect specific neural pathways. Supporting this concept, quantitative trait locus (QTL) analysis of mouse strains that show differential behavior in the TST and FST have mapped both distinct and common gene loci linked to behavior in these tests (Yoshikawa et al., 2002; Tomida et al., 2009).

One strain of genetically altered mice shown to have decreased immobility time (antidepressant effect) in the TST and FST are those with a specific deletion of the *Tac1* gene, encoding the neuropeptides Substance P (SP) and Neurokinin A (Bilkei-Gorzo et al., 2002). Tac1 mRNA, expression of which distinguishes the dMHb from the adjacent vMHb and LHb, is nearly absent in dMHb^{CKO} mice (Hsu et al., 2014). SP is also strongly expressed in dMHb fibers terminating in the lateral part of the interpeduncular nucleus in the ventral midbrain (Hsu et al., 2013). Thus it is possible that the decreased TST immobility time observed in dMHb^{CKO} mice results from a loss of *Tac1* peptide signaling in the habenulopeduncular system; the effect of *Tac1* gene deletion on the FST may reside in another pathway. NKB, the *Tac2* gene product co-expressed with SP in the dMHb and its terminal fibers in the IP, may also play a role in these effects, but little is known about the specific function of this peptide in the CNS.

dMHb^{CKO} mice show marked sensitization to the induction of learned helplessness. In contrast, ablation of the entire habenula attenuates the learned helplessness response (Amat et al., 2001), an effect which may be attributable to the LHb, since the induction of learned helplessness increases synaptic inputs to LHb neurons (Li et al., 2011). We expected to find that the sensitization to learned

helplessness in dMHb^{CKO} mice resulted from the marked loss of dMHb neurons in these animals. However, *Pou4f1*$^{+/-}$ mice, in which the dMHb is intact, also show sensitization to the induction of learned helplessness, demonstrating that *Pou4f1* haploinsufficiency is sufficient to produce this effect. None of the other behavioral paradigms tested were affected by *Pou4f1* haploinsufficiency.

The effect of *Pou4f1* haploinsufficiency on learned helplessness was not anticipated in the light of prior work on the role of this transcription factor in neural development and gene regulation. Independent null alleles of *Pou4f1* have been generated in at least three laboratories. Homozygous *Pou4f1* null mutants die shortly following birth, probably from defects in brainstem motor systems (McEvilly et al., 1996), but *Pou4f1* hemizygous mice are viable, fertile, and have no known developmental defects (McEvilly et al., 1996; Xiang et al., 1996; Quina et al., 2005). Furthermore, in the peripheral sensory nervous system, where Pou4f1 is a key developmental regulator, an autoregulatory mechanism has been identified which compensates for *Pou4f1* gene dosage in heterozygous null embryos, nearly normalizing the expression of downstream regulatory targets (Trieu et al., 2003; Eng et al., 2004). Pou4f1 is expressed in multiple CNS regions that are potential candidates for mediating the effect of haploinsufficiency on learned helplessness. These include the lateral habenula, superior colliculus (tectum), interpeduncular nucleus, red nucleus, and inferior olive (Fedtsova and Turner, 1995). Aside from the lateral habenula, however, the effect of these brain regions on mood regulation and stress response is not well characterized.

In a prior study we have shown that dMHb^{CKO} mice have markedly reduced voluntary wheel running activity (Hsu et al., 2014). This appears to be a specific deficit in exercise reinforcement, since basal locomotion is not affected. Although not generally used as a model of depression, WRA may interact with affective state and has been shown to produce an antidepressant-like effect in rats and mice (Greenwood et al., 2003; Duman et al., 2008). Thus we conclude that the dMHb circuit clearly intersects pathways for depression-related behaviors across multiple models. These results are broadly consistent with the role of the dMHb in exercise reinforcement and intracranial self-stimulation reinforcement. However, ablation of the dMHb does not simply cause depression-related behaviors, nor does it prevent them in a way that encompasses all of

the behavioral constructs used to model mood disorders and fear. As specific tools are used to dissect the underlying brain circuits for each of these mood-related behaviors, these pathways may be shown to impact depression-related behaviors by distinct mechanisms.

Figure legends

Figure 1. *Pou4f1* knockout models used for analysis of dMHb function. **(A)** Summary of genetic models used to generate dMHb lesions. **(B,C)** Coronal sections through the habenula at bregma -1.58mm were stained with antibodies for choline acetyltransferase (Chat) and either Pou4f1 (Brn3a protein) to reveal habenula neurons expressing this factor, or for the *lacZ* gene product βGal, expressed by the $Pou4f1^{tlacZ}$ allele, which allows the identification of neurons that would normally express Pou4f1 in cells in which the gene has been deleted. (B) $dMHb^{Ctrl}$ mouse with the genotype $Pou4f1^{flox/+}/Syt6^{Cre}$. Nuclear staining for Pou4f1 shows expression in both the vMHb and dMHb, and scattered expression in the LHb. The vMHb is distinguished by the expression of Chat, and the Pou4f1-positive, Chat-negative dMHb is circled. Scale bar = 100μm. (C) $dMHb^{CKO}$ mouse with the genotype $Pou4f1^{flox/tlacZ}/Syt6^{Cre}$. Staining for *lacZ* is used to show the extent of the dMHb lesion in the absence of Pou4f1 protein. The extent of the dMHb is greatly reduced (circle) and only a few LacZ-positive, Chat-negative neurons remain in the medial habenula. Neurons of the vMHb, distinguished by Chat expression in (A-B), are intact in both the $dMHb^{Ctrl}$ and $dMHb^{CKO}$ mice. The area within the dMHb that is not stained by any of the antibodies used consists of axon tracts of the striae medularis and/or habenula commissure.

Figure 2. Conditioned fear response in $dMHb^{CKO}$ mice. **(A)** Training session: Time spent in freezing behavior in one-minute intervals during 3 minutes of acclimation, followed by 6 intervals preceded by the delivery of a 1s shock, is shown. Shaded bar shows the period of shock administration. **(B)** Contextual conditioned fear response: On the testing day, the time spent in freezing behavior was assessed in the same environment as the training session, but without shock delivery, to evaluate the conditioned fear response. $dMHb^{CKO}$ and $dMHb^{Ctrl}$ mice exhibited the same amount of freezing during both the training and testing day. **(C)** Extinction of the conditioned fear response: Time spent in freezing behavior during three subsequent days of testing is shown. The conditioned fear response showed gradual extinction in the absence of further shock stimuli. * P = 0.033, ** P = 0.0082, *** P = 0.0003, and **** P < 0.0001,

609 significant difference between days for these genotypes. N = 12 dMHb^{Ctrl} and 10
610 dMHb^{CKO} mice.
611
612 **Figure 3. Learned helplessness assessed by active avoidance in dMHb^{CKO} mice.**
613 **(A)** Learned helplessness response: The mean latency to escape in the shuttle box
614 following one day of inescapable shock training, or exposure to the training chamber
615 without a shock, is shown. Both the dMHb^{CKO} and dMHb^{Ctrl} mice that received shocks
616 during training showed increased latency to escape, but dMHb^{CKO} mice exhibited a
617 stronger effect. ** $P < 0.01$, **** $P < 0.0001$ for difference between groups indicated. **(B)**
618 Persistence of the learned helplessness response: The mean latency to escape was
619 reassessed for the cohort shown in (A) 3 weeks after inescapable shock training.
620 dMHb^{Ctrl} mice that received inescapable shocks returned to near-baseline escape times.
621 dMHb^{CKO} mice that received inescapable shocks retained the learned helplessness
622 behavior. ** $P < 0.01$ and **** $P < 0.0001$, significant difference between groups. N =
623 13 no-shock dMHb^{Ctrl}, 10 shocked dMHb^{Ctrl}, 11 no-shock dMHb^{CKO}, and 17 shocked
624 dMHb^{CKO} mice. **(C)** Convergence of learned helplessness response with extended
625 training: The mean latency to escape was assessed after 3 days of inescapable shock
626 training in a different cohort of mice. Both the dMHb^{CKO} and dMHb^{Ctrl} mice received
627 shocks during the training. The prolonged training increased escape latency for both
628 genotypes when assessed by active avoidance one day after the final training session.
629 N = 11 dMHb^{Ctrl} and 9 dMHb^{CKO} mice. **(D,E)** Assessment of learned helplessness in a
630 separate cohort of *Pou4f1* hemizygous mice. (D) Learned helplessness response: The
631 mean latency to escape in the shuttle box following one day of inescapable shock
632 training is shown. Both the Pou4f1$^{+/-}$ and Pou4f1$^{+/+}$ (wild type) mice received shocks
633 during the training. Pou4f1$^{+/-}$ mice exhibited increased latency to escape relative to
634 Pou4f1$^{+/+}$ mice, i.e. were more susceptible to the induction of learned helplessness. **
635 $P = 0.0059$, significant difference between the genotypes. (E) Persistence of learned
636 helplessness response: The mean latency to escape was reassessed for the cohort
637 shown in (D) 3 weeks after inescapable shock training. The Pou4f1$^{+/-}$ mice showed
638 persistently elevated escape latency relative to Pou4f1$^{+/+}$ mice. *** $P = 0.0007$,
639 significant difference between the genotypes. Minor modifications to the active

avoidance protocol used in (D,E), resulting in somewhat longer escape times, are described in Methods.

Figure 4. Tail suspension test immobility time in dMHb^{CKO} and Pou4f1 hemizygous mice, and affect of hemizygosity on rotarod performance. **(A)** Time spent immobile in the TST is shown for dMHb^{CKO} and dMHb^{Ctrl} mice. ** P < 0.01, significance difference between the genotypes. N = 11 dMHb^{Ctrl} and 9 dMHb^{CKO} mice. **(B)** Time spent immobile in the TST is shown for Pou4f1$^{+/+}$ and Pou4f1$^{+/-}$ mice. Pou4f1 gene dosage did not affect immobility time in the absence of a developmental dMHb lesion. N = 16 Pou4f1$^{+/+}$ and 16 Pou4f1$^{+/-}$ mice. Pou4f1$^{+/-}$ mice have the genotype *Pou4f1$^{+/tlacZ}$*. **(C)** Rotarod performance is not affected in Pou4f1$^{+/-}$ mice. Both the Pou4f1$^{+/-}$ and Pou4f1$^{+/+}$ mice had similar latency to fall times in this test. N = 16 of each genotype.

Figure 5. Specific expression of channelrhodopsin in tachykinin-expressing neurons in dMHb-Tac^{ChR2} mice. **(A,B)** Comparison of Tac1 and Tac2 mRNA expression in the habenula; the axial level is approximately bregma -1.6mm. Data are derived from the Allen Mouse Brain Atlas. **(C, D)** Conditional expression of ChR2-eYFP in Ai32 mice driven by Tac2^{IRESCre} in the habenula. Dashed lines demarcate the extent of the habenula based on the expression of the nuclear factor Pou4f1 (C). Expression is infrequently seen in the vMHb, as defined by the expression of Chat (D). **(E)** Conditional expression of tdTomato mRNA in Ai14 mice driven by Tac2^{IRESCre} in the habenula (Allen Transgenic Mouse Characterization Project). **(F-H)** ChR2-eYFP labeled fibers terminate predominantly in the lateral part of the interpeduncular nucleus, which receives afferents from the dMHb (F,H); these fibers are largely excluded from the IPR/IPC, which receive fibers mainly from the vMHb (G). **(I-J)** Co-localization of substance P, product of the Tac1 gene, with ChR2-eYFP in the interpeduncular nucleus of dMHb-Tac^{ChR2} mice. **(K)** Co-localization of neurokinin B, product of the Tac2 gene, with ChR2-eYFP. dMHb, dorsal medial habenula; IPC, IPL, IPR, interpeduncular nucleus, caudal, lateral, and rostral parts; LHb, lateral habenula; vMHb, ventral medial habenula. Scale: A, 200μm; C,F,I, 100μm; J, 50μm.

Figure 6. Intrinsic reinforcement mediated by neurokinin-expressing dMHb neurons. **(A,B)** Light entrainment of dMHb neurons expressing $Tac2^{Cre}$-driven ChR2. **(C)** Optogenetic ICSS in $dMHb^{ChR2}$ mice. Two nosepoke receptacles in each behavioral compartment were randomized to active and inactive at the beginning of the trial. The initial assignment was maintained for days 1-4 of training, then reversed for days 5-8 of training (reversal trials). Mice received a 2-second light stimulation of the dMHb for each nosepoke event in the active receptacle. **(D)** ICSS in control mice lacking a Cre-driver; no preference for the active receptacle was observed. **(E)** ICSS in $vMHb^{ChR2}$ mice; no preference was observed. **(F)** Average values for nosepoke events in the inactive and active receptacles over four days of trials for $dMHb^{ChR2}$ (N=7), $vMHb^{ChR2}$ (N=6) and control (N=11) mice.

Figure 7 Placement of optical fibers in ICSS experimental mice. Mice with bilateral implanted fiber optic cannulas were perfused with a fixative at the conclusion of behavioral experiments and brains were examined for cannula placement. Fiber termini are shown on the level of a standard anatomical map (Paxinos and Franklin, 2001) closest to their rostrocaudal position at bregma -1.34, 1.46, 1.58, or 1.70 mm. Nearly all of the cannulas thus were positioned within ±0.2mm of the intended coordinates at bregma- 1.6mm. Although some cannulas were displaced laterally, at least one of the two optical fibers termiated close to the habenula in every case.

Fibers for $dMHb^{ChR2}$ mice are shown in red, $vMHb^{ChR2}$ mice are shown in green, and control mice are shown in blue. Connected dots indicate the probable ventral termini of the optical fibers from each case. In some cases, the right and left optical fibers mapped most accurately to different planes of section and are shown by disconnected dots. If the cannula track could not be followed to the terminus of the optical fiber, for instance due to termination in the ventricle, the most ventral position and the direction of the cannula track observed are indicated by an arrow. In all cases, the optical fibers were intact and transmitted light efficiently when examined postmortem after the experimental protocol. Scale bar, 0.5 mm.

Light was delivered through the bilateral cannula for a total output of 8mW, corresponding to 4mW per 100μm fiber or 509mW/mm^2 at the fiber teriminus. Because some of the cannulas were displaced laterally, we used a published empirically-derived model for the diffusion of 473nm light in the mouse brain tissue to estimate the light intensity at target structures (Yizhar et al., 2011). The example laterally displaced cannula pair is indicated by an asterisk (Bregma 1.46 view). The boundary of light penetration at 1% of that delivered at the fiber terminus is indicated by a dashed line (~5mw/mm^2). Although one cannula is displaced laterally, the medial cannula is predicted to illuminate the entire habenula. The predicted intensity of light, 5mW/mm^2, is sufficient to elicit reliable action potentials from dMHb neurons in brain slice preparations.

Figure 8. Real-time place preference. RTPP studies were conducted in a two-chamber place-preference box in which mice received light stimulation in one side, and could move freely between compartments. **(A, B)** Example activity traces of control (A) and dMHb^{ChR2} (B) mice. Data are shown for an entire 15 minute trial fo a single animal of each genotype. **(C,D)** Side preference of control (C, n=8) and dMHb^{ChR2} mice (D, n=8) displayed in 5 minute bins over the course of a 15 minute trial. The large variability in the side occupancy in the later intervals is likely to represent decreasing exploration during the course of the trial, with individual mice settling on one side of the chamber or the other, apparently without preference. **(E)** Summary of side occupancy for 15 minute trial. No significant effect of side or genotype was observed.

References

Amat J, Sparks PD, Matus-Amat P, Griggs J, Watkins LR, Maier SF (2001) The role of the habenular complex in the elevation of dorsal raphe nucleus serotonin and the changes in the behavioral responses produced by uncontrollable stress. Brain Res 917:118-126.

Bilkei-Gorzo A, Racz I, Michel K, Zimmer A (2002) Diminished anxiety- and depression-related behaviors in mice with selective deletion of the Tac1 gene. J Neurosci 22:10046-10052.

Chourbaji S, Zacher C, Sanchis-Segura C, Dormann C, Vollmayr B, Gass P (2005) Learned helplessness: validity and reliability of depressive-like states in mice. Brain Res Brain Res Protoc 16:70-78.

Cryan JF, Mombereau C (2004) In search of a depressed mouse: utility of models for studying depression-related behavior in genetically modified mice. Mol Psychiatry 9:326-357.

Cryan JF, Mombereau C, Vassout A (2005) The tail suspension test as a model for assessing antidepressant activity: review of pharmacological and genetic studies in mice. Neurosci Biobehav Rev 29:571-625.

Dejean C, Courtin J, Rozeske RR, Bonnet MC, Dousset V, Michelet T, Herry C (2015) Neuronal Circuits for Fear Expression and Recovery: Recent Advances and Potential Therapeutic Strategies. Biol Psychiatry 78:298-306.

Duman CH (2010) Models of depression. Vitam Horm 82:1-21.

Duman CH, Schlesinger L, Russell DS, Duman RS (2008) Voluntary exercise produces antidepressant and anxiolytic behavioral effects in mice. Brain Res 1199:148-158.

Eng SR, Lanier J, Fedtsova N, Turner EE (2004) Coordinated regulation of gene expression by Brn3a in developing sensory ganglia. Development 131:3859-3870.

Fedtsova N, Turner E (1995) Brn-3.0 Expression identifies early post-mitotic CNS neurons and sensory neural precursors. Mechanisms of Development 53:291-304.

Gerfen CR, Paletzki R, Heintz N (2013) GENSAT BAC cre-recombinase driver lines to study the functional organization of cerebral cortical and basal ganglia circuits. Neuron 80:1368-1383.

Greenwood BN, Foley TE, Day HE, Campisi J, Hammack SH, Campeau S, Maier SF, Fleshner M (2003) Freewheel running prevents learned helplessness/behavioral depression: role of dorsal raphe serotonergic neurons. J Neurosci 23:2889-2898.

Harris JA, Hirokawa KE, Sorensen SA, Gu H, Mills M, Ng LL, Bohn P, Mortrud M, Ouellette B, Kidney J, Smith KA, Dang C, Sunkin S, Bernard A, Oh SW, Madisen L, Zeng H (2014) Anatomical characterization of Cre driver mice for neural circuit mapping and manipulation. Front Neural Circuits 8:76.

Heldt SA, Ressler KJ (2006) Lesions of the habenula produce stress- and dopamine-dependent alterations in prepulse inhibition and locomotion. Brain Res 1073-1074:229-239.

Hikosaka O (2010) The habenula: from stress evasion to value-based decision-making. Nat Rev Neurosci 11:503-513.

Hsu YW, Tempest L, Quina LA, Wei AD, Zeng H, Turner EE (2013) Medial Habenula Output Circuit Mediated by alpha5 Nicotinic Receptor-Expressing GABAergic Neurons in the Interpeduncular Nucleus. J Neurosci 33:18022-18035.

Hsu YW, Wang SD, Wang S, Morton G, Zariwala HA, de la Iglesia HO, Turner EE (2014) Role of the dorsal medial habenula in the regulation of voluntary activity, motor function, hedonic state, and primary reinforcement. J Neurosci 34:11366-11384.

Keifer OP, Jr., Hurt RC, Ressler KJ, Marvar PJ (2015) The Physiology of Fear: Reconceptualizing the Role of the Central Amygdala in Fear Learning. Physiology (Bethesda) 30:389-401.

Lammel S, Lim BK, Ran C, Huang KW, Betley MJ, Tye KM, Deisseroth K, Malenka RC (2012) Input-specific control of reward and aversion in the ventral tegmental area. Nature 491:212-217.

773 Lecourtier L, Kelly PH (2007) A conductor hidden in the orchestra? Role of the habenular complex in
774 monoamine transmission and cognition. Neurosci Biobehav Rev 31:658-672.
775 Li B, Piriz J, Mirrione M, Chung C, Proulx CD, Schulz D, Henn F, Malinow R (2011) Synaptic potentiation
776 onto habenula neurons in the learned helplessness model of depression. Nature 470:535-539.
777 Li K, Zhou T, Liao L, Yang Z, Wong C, Henn F, Malinow R, Yates JR, 3rd, Hu H (2013) betaCaMKII in lateral
778 habenula mediates core symptoms of depression. Science 341:1016-1020.
779 Madisen L et al. (2012) A toolbox of Cre-dependent optogenetic transgenic mice for light-induced
780 activation and silencing. Nat Neurosci 15:793-802.
781 Maier SF (1984) Learned helplessness and animal models of depression. Prog Neuropsychopharmacol
782 Biol Psychiatry 8:435-446.
783 Maier SF, Watkins LR (2005) Stressor controllability and learned helplessness: the roles of the dorsal
784 raphe nucleus, serotonin, and corticotropin-releasing factor. Neurosci Biobehav Rev 29:829-841.
785 Mar L, Yang FC, Ma Q (2012) Genetic marking and characterization of Tac2-expressing neurons in the
786 central and peripheral nervous system. Mol Brain 5:3.
787 Maren S, Phan KL, Liberzon I (2013) The contextual brain: implications for fear conditioning, extinction
788 and psychopathology. Nat Rev Neurosci 14:417-428.
789 Masugi M, Yokoi M, Shigemoto R, Muguruma K, Watanabe Y, Sansig G, van der Putten H, Nakanishi S
790 (1999) Metabotropic glutamate receptor subtype 7 ablation causes deficit in fear response and
791 conditioned taste aversion. J Neurosci 19:955-963.
792 Matsumoto M, Hikosaka O (2009) Representation of negative motivational value in the primate lateral
793 habenula. Nat Neurosci 12:77-84.
794 McEvilly RJ, Erkman L, Luo L, Sawchenko PE, Ryan AF, Rosenfeld MG (1996) Requirement for Brn-3.0 in
795 differentiation and survival of sensory and motor neurons. Nature 384:574-577.
796 Pham J, Cabrera SM, Sanchis-Segura C, Wood MA (2009) Automated scoring of fear-related behavior
797 using EthoVision software. J Neurosci Methods 178:323-326.
798 Proulx CD, Hikosaka O, Malinow R (2014) Reward processing by the lateral habenula in normal and
799 depressive behaviors. Nat Neurosci 17:1146-1152.
800 Quina LA, Wang S, Ng L, Turner EE (2009) Brn3a and Nurr1 mediate a gene regulatory pathway for
801 habenula development. J Neurosci 29:14309-14322.
802 Quina LA, Pak W, Lanier J, Banwait P, Gratwick K, Liu Y, Velasquez T, O'Leary DD, Goulding M, Turner EE
803 (2005) Brn3a-expressing retinal ganglion cells project specifically to thalamocortical and
804 collicular visual pathways. J Neurosci 25:11595-11604.
805 Rossi J, Balthasar N, Olson D, Scott M, Berglund E, Lee CE, Choi MJ, Lauzon D, Lowell BB, Elmquist JK
806 (2011) Melanocortin-4 receptors expressed by cholinergic neurons regulate energy balance and
807 glucose homeostasis. Cell Metab 13:195-204.
808 Rozeske RR, Valerio S, Chaudun F, Herry C (2015) Prefrontal neuronal circuits of contextual fear
809 conditioning. Genes Brain Behav 14:22-36.
810 Soria-Gomez E, Busquets-Garcia A, Hu F, Mehidi A, Cannich A, Roux L, Louit I, Alonso L, Wiesner T,
811 Georges F, Verrier D, Vincent P, Ferreira G, Luo M, Marsicano G (2015) Habenular CB1 Receptors
812 Control the Expression of Aversive Memories. Neuron 88:306-313.
813 Stamatakis AM, Stuber GD (2012) Activation of lateral habenula inputs to the ventral midbrain promotes
814 behavioral avoidance. Nat Neurosci 15:1105-1107.
815 Steru L, Chermat R, Thierry B, Simon P (1985) The tail suspension test: a new method for screening
816 antidepressants in mice. Psychopharmacology (Berl) 85:367-370.
817 Tomida S, Mamiya T, Sakamaki H, Miura M, Aosaki T, Masuda M, Niwa M, Kameyama T, Kobayashi J,
818 Iwaki Y, Imai S, Ishikawa A, Abe K, Yoshimura T, Nabeshima T, Ebihara S (2009) Usp46 is a
819 quantitative trait gene regulating mouse immobile behavior in the tail suspension and forced
820 swimming tests. Nat Genet 41:688-695.

821 Trieu M, Ma A, Eng SR, Fedtsova N, Turner EE (2003) Direct autoregulation and gene dosage
822 compensation by POU-domain transcription factor Brn3a. Development 130:111-121.
823 Xiang M, Zhou L, Nathans J (1996) Similarities and differences among inner retinal neurons revealed by
824 the expression of reporter transgenes controlled by Brn-3a, Brn-3b, and Brn-3c promotor
825 sequences. Vis Neurosci 13:955-962.
826 Yamaguchi T, Danjo T, Pastan I, Hikida T, Nakanishi S (2013) Distinct roles of segregated transmission of
827 the septo-habenular pathway in anxiety and fear. Neuron 78:537-544.
828 Yizhar O, Fenno LE, Davidson TJ, Mogri M, Deisseroth K (2011) Optogenetics in neural systems. Neuron
829 71:9-34.
830 Yoshikawa T, Watanabe A, Ishitsuka Y, Nakaya A, Nakatani N (2002) Identification of multiple genetic loci
831 linked to the propensity for "behavioral despair" in mice. Genome Res 12:357-366.
832
833

A

Genotype	Number of *Pou4f1* copies		dMHb status	Abbreviation
	dMHb	elsewhere		
Pou4f1$^{tlacZ/flox}$, Syt6$^{Cre/+}$	Zero	One	Lesioned	dMHb^{CKO}
Pou4f1$^{flox/+}$, Syt6$^{Cre/+}$	One	Two	Intact	dMHb^{Ctrl}
Pou4f1$^{tlacZ/+}$, Syt6$^{Cre/+}$	One	One	Intact	Pou4f1$^{+/-}$
Pou4f1$^{+/+}$, Syt6$^{Cre/+}$	Two	Two	Intact	Pou4f1$^{+/+}$
C57Bl/6	Two	Two	Intact	WT

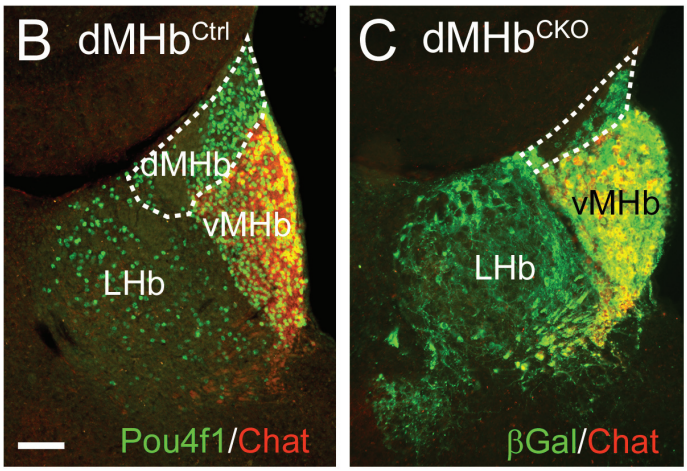

Hsu, et al., Figure 1

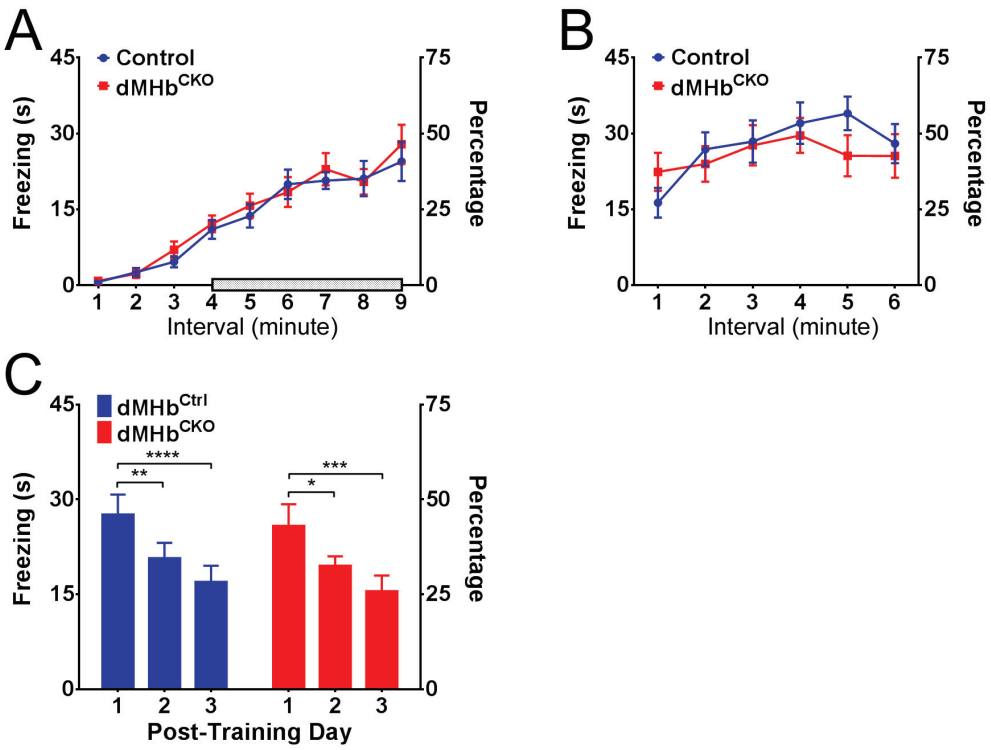

Hsu, et al., Figure 2

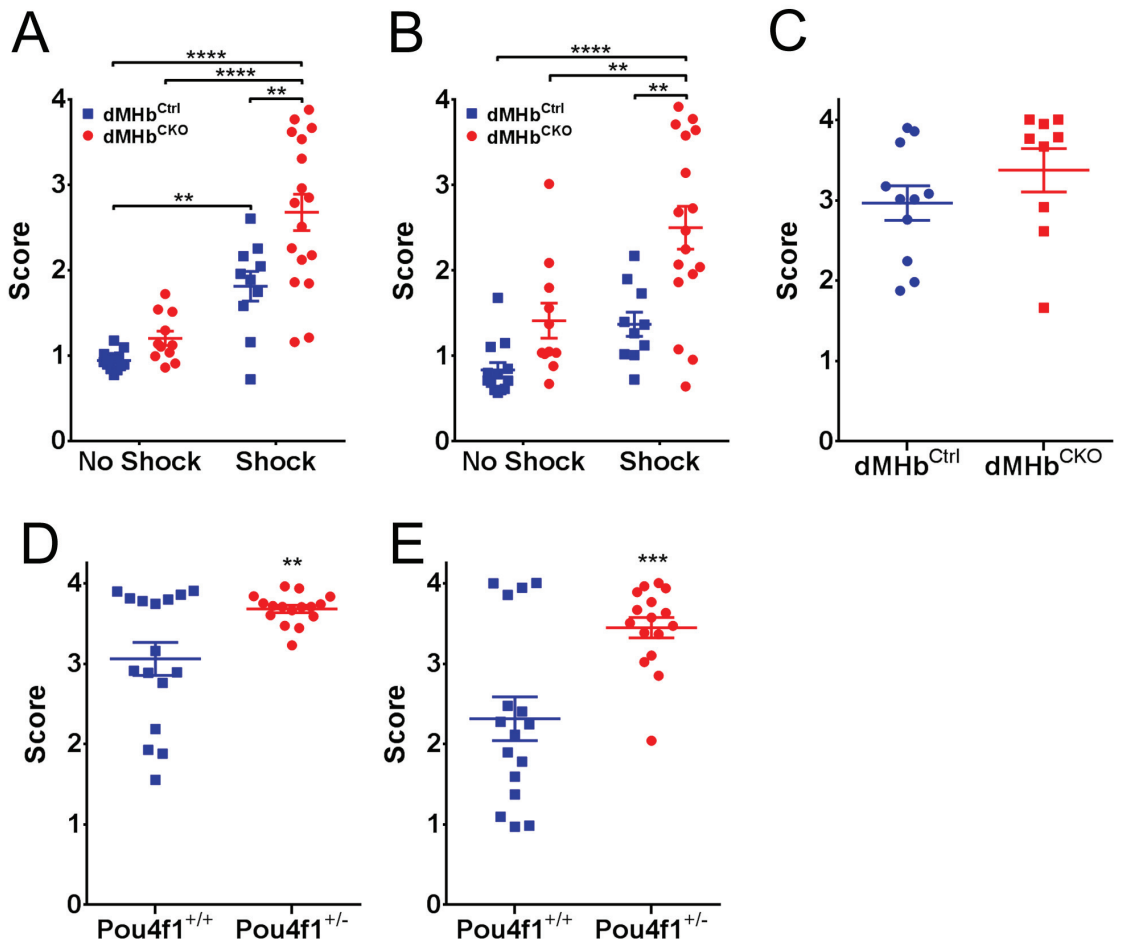

Hsu, et al., Figure 3

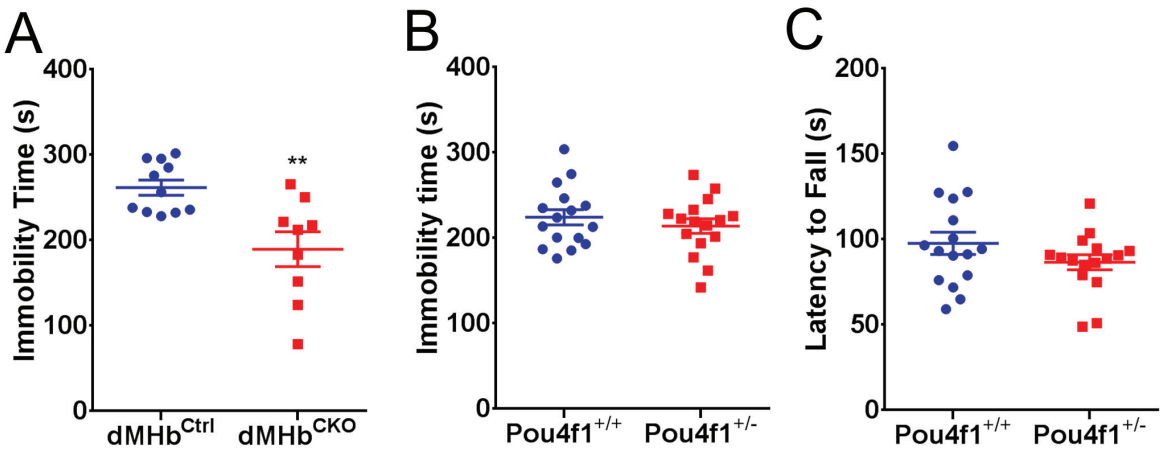

Hsu, et al., Figure 4

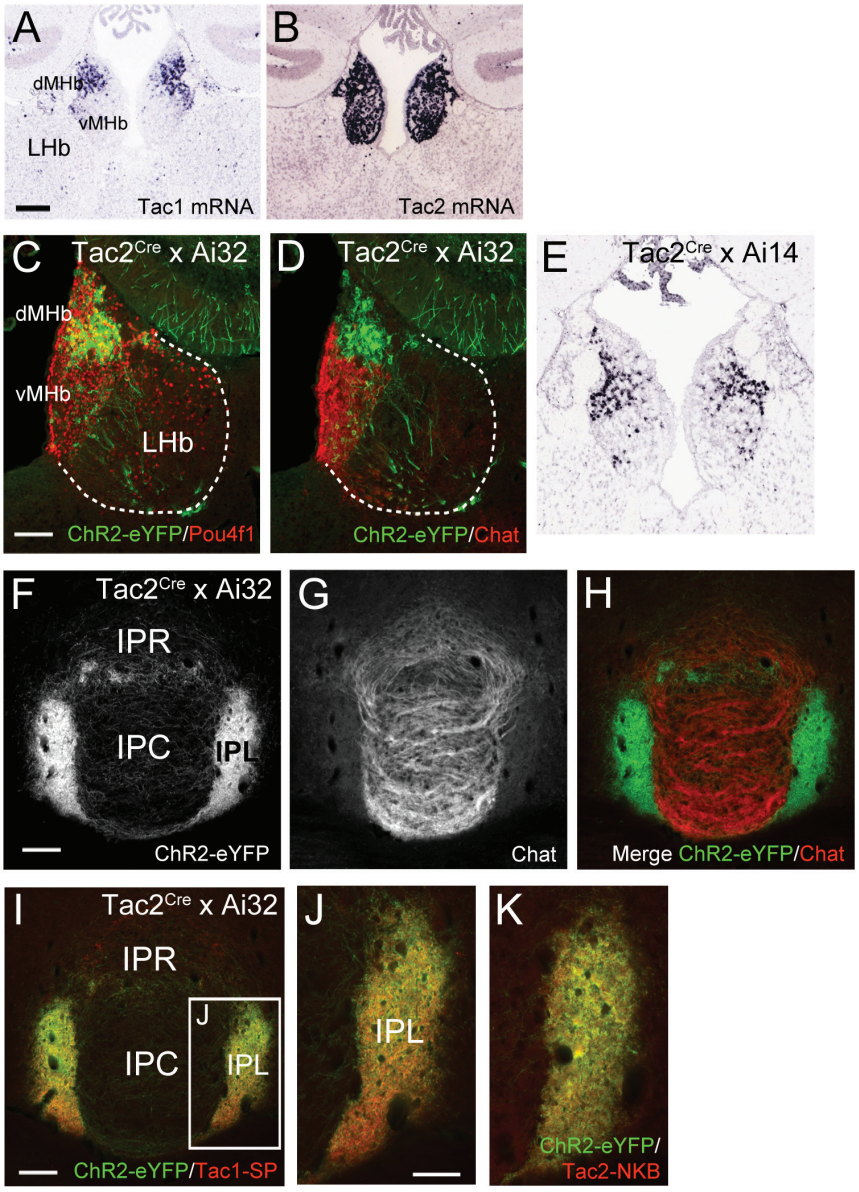

Hsu, et al., Figure 5

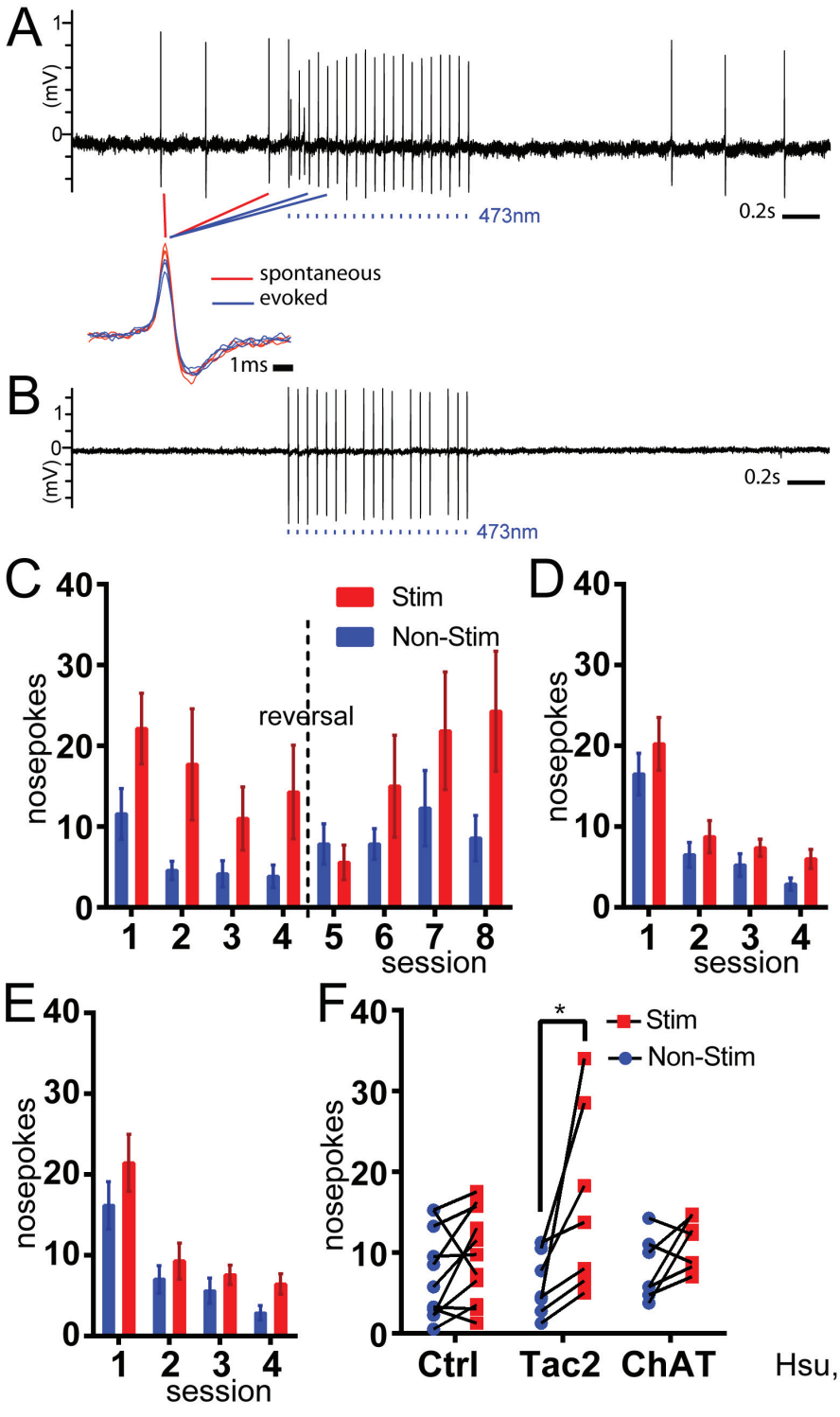

Hsu, et al., Figure 6

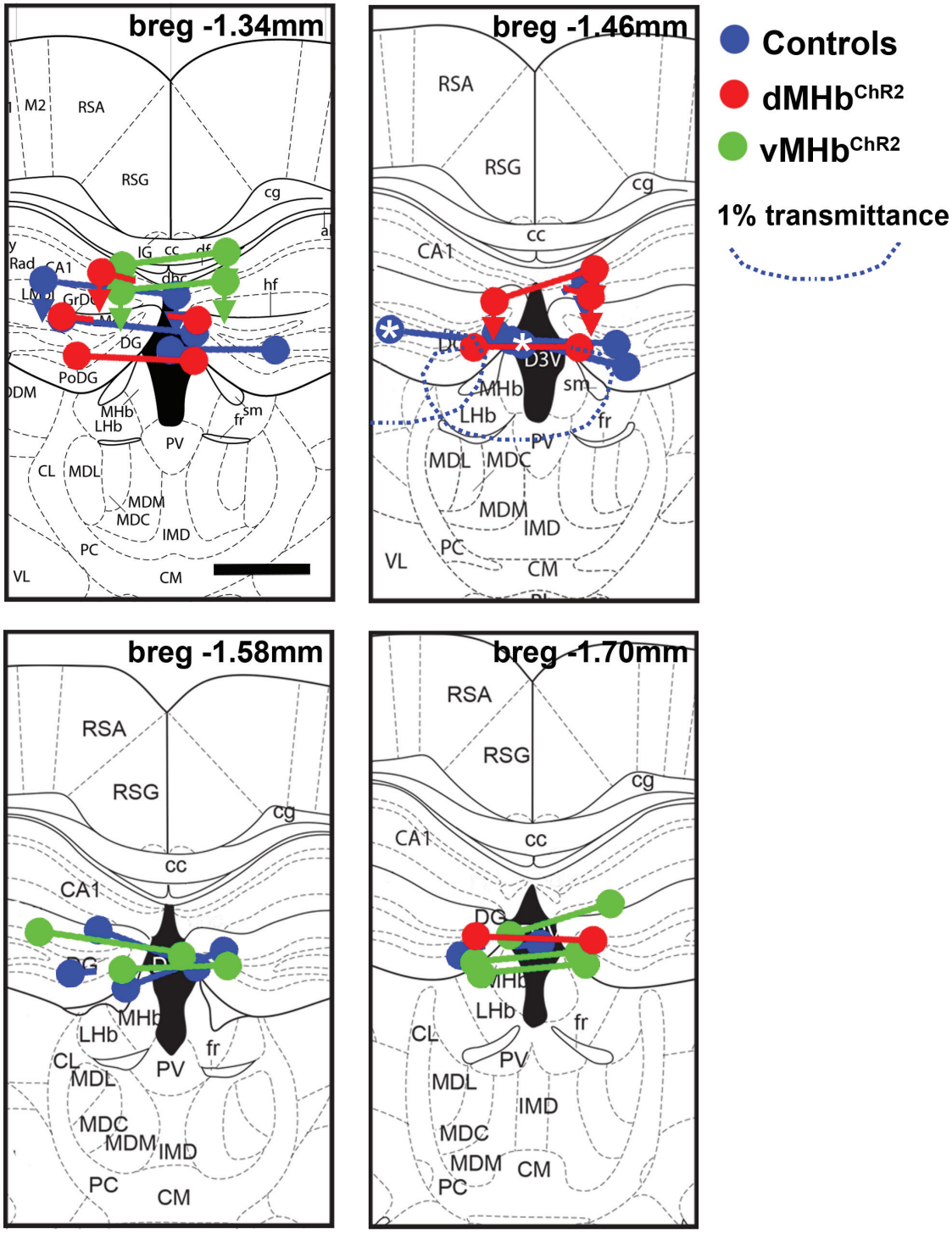

Hsu, et al., Figure 7

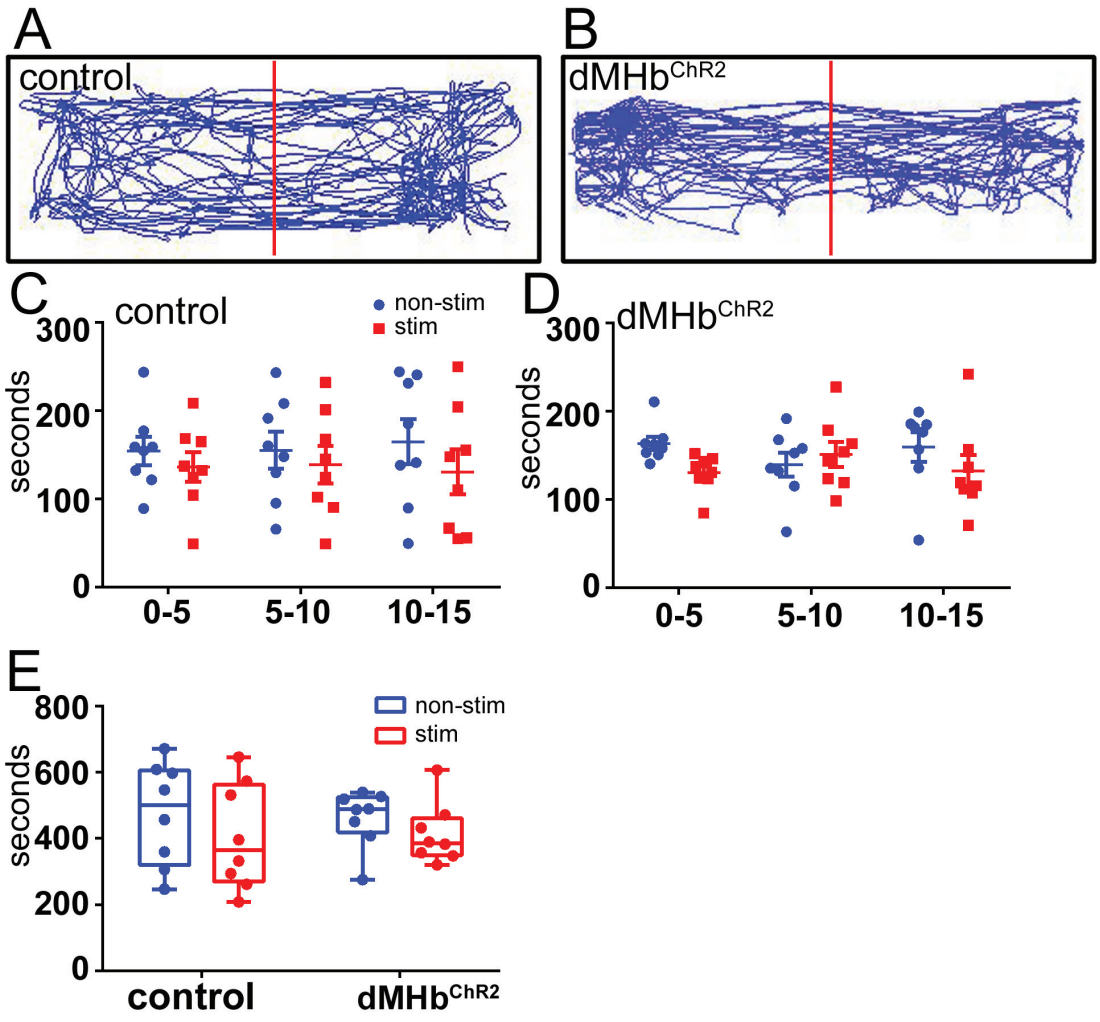

Hsu, et al., Figure 8